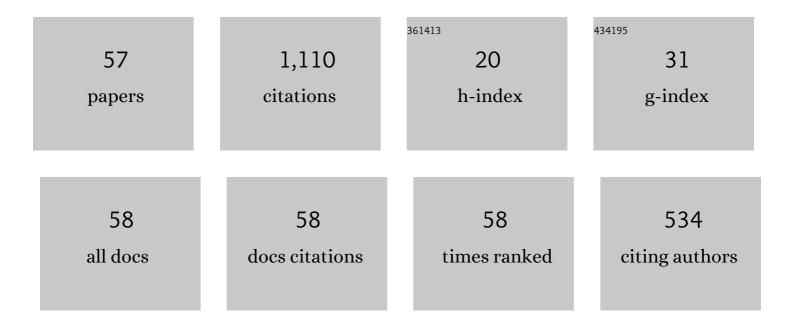
List of Publications by Year in descending order

Source: https://exaly.com/author-pdf/6500976/publications.pdf Version: 2024-02-01



LIN SONC

| # | Article | IF | CITATIONS |
|----|---|------------------|-----------|
| 1 | Hydrogen absorption/desorption cycling performance of Mg-based alloys with in-situ formed Mg2Ni and LaH (xÂ=Â2, 3) nanocrystallines. Journal of Magnesium and Alloys, 2023, 11, 1180-1192. | 11.9 | 16 |
| 2 | Deformation and phase transformation behaviors of a high Nb-containing TiAl alloy compressed at intermediate temperatures. Journal of Materials Science and Technology, 2022, 102, 89-96. | 10.7 | 18 |
| 3 | xmins:mmi="http://www.w3.org/1998/Math/Math/MathML" altimg="si11.svg"> <mmi:msub><mmi:mrow /><mmi:mover accent="true"><mmi:mn>2</mmi:mn><mmi:mo>Â⁻</mmi:mo></mmi:mover </mmi:mrow </mmi:msub> 1}<< xmlns:mml="http://www.w3.org/1998/Math/MathML" altimg="si12.svg"> <mmi:msub><mmi:mrow< td=""><td>mmbmath</td><td>11</td></mmi:mrow<></mmi:msub> | m mb math | 11 |
| 4 | Mechanisms of hydrides' nucleation and the effect of hydrogen pressure induced driving force on de-/hydrogenation kinetics of Mg-based nanocrystalline alloys. International Journal of Hydrogen Energy, 2022, 47, 1063-1075. | 7.1 | 8 |
| 5 | Ameliorated microstructure and hydrogen absorption/desorption properties of novel Mg–Ni–La alloy doped with MWCNTs and Co nanoparticles. International Journal of Hydrogen Energy, 2022, 47, 18044-18057. | 7.1 | 4 |
| 6 | In- and ex-situ study of the deformation behavior of the βo(ωo) phase in a Ti4Al3Nb alloy during high-temperature compression. Journal of Alloys and Compounds, 2022, , 165626. | 5.5 | 1 |
| 7 | Experimental Phase Equilibria and Isopleth Section of 8Nb-TiAl Alloys. Metals, 2021, 11, 1229. | 2.3 | 6 |
| 8 | Creep-induced ωo phase precipitation and cavity formation in a cast 45.5Ti-45Al-9Nb-0.5B alloy. Journal of Alloys and Compounds, 2021, 875, 160106. | 5.5 | 7 |
| 9 | On the reversibility of the α2/ï‰o phase transformation in a high Nb containing TiAl alloy during high temperature deformation. Journal of Materials Science and Technology, 2021, 93, 96-102. | 10.7 | 6 |
| 10 | Microstructure and phase transformations of ï‰o-Ti4Al3Nb based alloys after quenching and subsequent aging at intermediate temperatures. Journal of Alloys and Compounds, 2020, 821, 153387. | 5.5 | 11 |
| 11 | Precipitation of nanocrystalline LaH3 and Mg2Ni and its effect on de-/hydrogenation thermodynamics of Mg-rich alloys. International Journal of Hydrogen Energy, 2020, 45, 32221-32233. | 7.1 | 17 |
| 12 | Tunable microstructure, de-/hydrogenation kinetics and thermodynamics performance of Mg–Ni–La–Ti–H systems. International Journal of Hydrogen Energy, 2020, 45, 6701-6712. | 7.1 | 3 |
| 13 | New insights into high-temperature deformation and phase transformation mechanisms of lamellar structures in high Nb-containing TiAl alloys. Acta Materialia, 2020, 186, 575-586. | 7.9 | 65 |
| 14 | Microstructure evolution and enhanced creep property of a high Nb containing TiAl alloy with carbon addition. Journal of Alloys and Compounds, 2019, 807, 151649. | 5.5 | 30 |
| 15 | Identification of Laves phases in a Zr or Hf containing γ-γ′ Co-base superalloy. Journal of Alloys and Compounds, 2019, 805, 880-886. | 5.5 | 12 |
| 16 | Microstructure, phase stability and element partitioning of γ-γ′ Co-9Al-9W-2X alloys in different annealing conditions. Journal of Alloys and Compounds, 2019, 787, 594-605. | 5.5 | 23 |
| 17 | Composition dependent microstructure evolution, activation and de-/hydrogenation properties of Mg–Ni–La alloys. International Journal of Hydrogen Energy, 2019, 44, 16745-16756. | 7.1 | 24 |
| 18 | Corrosion resistance and interfacial morphologies of a high Nb-containing TiAl alloy with and without thermal barrier coatings in molten salts. Corrosion Science, 2019, 156, 139-146. | 6.6 | 22 |

| # | Article | IF | CITATIONS |
|----|---|-----|-----------|
| 19 | Microstructural evolution and hydrogen storage properties of a Ni-modified Mg15Al alloy. International Journal of Hydrogen Energy, 2019, 44, 10788-10799. | 7.1 | 12 |
| 20 | Evidence for deformation twinning of the D019-α2 phase in a high Nb containing TiAl alloy. Intermetallics, 2019, 109, 91-96. | 3.9 | 25 |
| 21 | Microstructure and absorption/desorption kinetics evolutions of Mg Ni Ce alloys during hydrogenation and dehydrogenation cycles. International Journal of Hydrogen Energy, 2018, 43, 8404-8414. | 7.1 | 19 |
| 22 | Hydride formation during cathodic charging and its effect on mechanical properties of a high Nb containing TiAl alloy. International Journal of Hydrogen Energy, 2018, 43, 8161-8169. | 7.1 | 10 |
| 23 | Precipitation behavior of ωo phase and texture evolution of a forged Ti-45Al-8.5Nb-(W, B, Y) alloy during creep. Materials Characterization, 2018, 136, 41-51. | 4.4 | 22 |
| 24 | Nucleation behavior of ωo phase in TiAl alloys at different elevated temperatures. Journal of Materials Science, 2018, 53, 5287-5295. | 3.7 | 5 |
| 25 | Coupling effects of deformation and thermal exposure on the precipitation behaviors of β o (ω) phases in a high Nb-containing TiAl alloy. Materials and Design, 2018, 148, 135-144. | 7.0 | 12 |
| 26 | Pressure Effect on Elastic Constants and Related Properties of Ti3Al Intermetallic Compound: A First-Principles Study. Materials, 2018, 11, 2015. | 2.9 | 46 |
| 27 | First-Principles Calculations on Structural Property and Anisotropic Elasticity of γ1-Ti4Nb3Al9 under Pressure. Materials, 2018, 11, 2025. | 2.9 | 2 |
| 28 | A comparative first-principles study of tetragonal TiAl and Ti4Nb3Al9 intermetallic compounds. Intermetallics, 2018, 101, 72-80. | 3.9 | 13 |
| 29 | Microstructure Evolution of a Ti-45Al-8.5Nb-0.2W-0.2B-0.02Y Alloy during Massive Transformation and Subsequent Annealing. Metals, 2018, 8, 89. | 2.3 | 2 |
| 30 | Evolution of B2(ω) region in high-Nb containing TiAl alloy in intermediate temperature range. Intermetallics, 2017, 82, 32-39. | 3.9 | 30 |
| 31 | Quantitative study of surface relief produced by formation of lamellar microstructure in a Î ³ -TiAl based alloy. Materials Letters, 2017, 188, 134-137. | 2.6 | 6 |
| 32 | Precipitation behavior of the ωo phase in an annealed high Nb-TiAl alloy. Journal of Alloys and Compounds, 2017, 701, 882-891. | 5.5 | 22 |
| 33 | In situ Observation of the Initial Stage of <i>γ</i> Lamella Formation in Ti48Al2Cr2Nb Alloy. Advanced Engineering Materials, 2017, 19, 1600670. | 3.5 | 2 |
| 34 | Alloying Effects on the Phase Transformation Behaviors of the Orthorhombic and Ordered ï‰ Phases in High Nb – TiAl Alloys. Advanced Engineering Materials, 2017, 19, 1700040. | 3.5 | 2 |
| 35 | Microstructure and hydrogen storage properties of Mg-Ni-Ce alloys with a long-period stacking ordered phase. Journal of Power Sources, 2017, 338, 91-102. | 7.8 | 62 |
| 36 | Ordinary dislocation configurations in high Nb-containing TiAl alloy deformed at high temperatures. Philosophical Magazine, 2017, 97, 515-526. | 1.6 | 5 |

| # | Article | IF | CITATIONS |
|----|--|-------------------|-----------|
| 37 | Air-stable MgH 2 â^ CeO 2 composite with facilitated de/hydrogenation kinetics synthesized by high energy ball milling. Materials Characterization, 2017, 133, 94-101. | 4.4 | 32 |
| 38 | Precipitation behavior of α2 phase in Ti–34Al–13Nb alloy. Journal of Alloys and Compounds, 2017, 725, 155-162. | 5.5 | 8 |
| 39 | Atomic-scale observations of B2 → ï‰-related phases transition in high-Nb containing TiAl alloy. Materials Characterization, 2017, 130, 135-138. | 4.4 | 14 |
| 40 | Dehydrogenation steps and factors controlling desorption kinetics of a Mg Ce hydrogen storage alloy. International Journal of Hydrogen Energy, 2017, 42, 21121-21130. | 7.1 | 22 |
| 41 | The Third-Order Elastic Moduli and Debye Temperature of SrFe2As2 and BaFe2As2: a First-Principles Study. Journal of Superconductivity and Novel Magnetism, 2017, 30, 1749-1756. | 1.8 | 10 |
| 42 | Precipitation behaviors in a quenched high Nb-containing TiAl alloy during annealing. Intermetallics, 2017, 89, 79-85. | 3.9 | 16 |
| 43 | Phase transformation mechanisms in a quenched Ti-45Al-8.5Nb-0.2W-0.2B-0.02YÂalloy after subsequentÂannealingÂatÂ800°C. Journal of Alloys and Compounds, 2017, 691, 60-66. | 5.5 | 29 |
| 44 | Effects of trace alloying elements on the phase transformation behaviors of ordered ω phases in high Nb-TiAl alloys. Materials and Design, 2017, 113, 47-53. | 7.0 | 39 |
| 45 | Precipitation Behavior of ωo Phase in Ti-37.5Al-12.5Nb Alloy. Metals, 2017, 7, 192. | 2.3 | 2 |
| 46 | Ab Initio Study of the Elastic and Mechanical Properties of B19 TiAl. Crystals, 2017, 7, 39. | 2.2 | 35 |
| 47 | Phase transformations in Ti–34Al–13Nb alloy. Journal of Materials Science, 2016, 51, 10478-10486. | 3.7 | 4 |
| 48 | Ordered ω phase transformations in Ti-45Al-8.5Nb-0.2B alloy. Intermetallics, 2015, 65, 22-28. | 3.9 | 30 |
| 49 | Ϊ‰o phase precipitation in annealed high Nb containing TiAl alloys. Progress in Natural Science: Materials International, 2015, 25, 147-152. | 4.4 | 7 |
| 50 | Deformation behaviour and 6H-LPSO structure formation at nanoindentation in lamellar high Nb containing TiAl alloy. Philosophical Magazine Letters, 2015, 95, 85-91. | 1.2 | 11 |
| 51 | Precipitates in high-Nb TiAl alloyed with Si. Materials Letters, 2015, 154, 8-11. | 2.6 | 13 |
| 52 | Ordered α2 to ωo phase transformations in high Nb-containing TiAl alloys. Acta Materialia, 2015, 91, 330-339. | 7.9 | 68 |
| 53 | B19 phase in Ti–45Al–8.5Nb–0.2W–0.2B–0.02Y alloy. Journal of Alloys and Compounds, 2015, 618, 3 | 30 5-3 10. | 20 |
| 54 | Cooling rate effects on the microstructure evolution in the βo zones of cast Ti–45Al–8.5Nb–(W, B, Y) alloy. Materials Characterization, 2014, 93, 62-67. | 4.4 | 38 |

| # | Article | IF | CITATIONS |
|----|---|-----|-----------|
| 55 | Phase transformation and decomposition mechanisms of the β (ω) phase in cast high Nb containing TiAl alloy. Journal of Alloys and Compounds, 2014, 616, 483-491. | 5.5 | 61 |
| 56 | Omega phase in as-cast high-Nb-containing TiAl alloy. Scripta Materialia, 2013, 68, 929-932. | 5.2 | 70 |
| 57 | The Microstructure and Compression Behavior of Multi-Step Forging Ti-45Al-8Nb Alloy after Annealing at 1100 °C. Materials Science Forum, 0, 747-748, 111-114. | 0.3 | Ο |